

18 **Abstract**

19 Seasonal forecasts are commonly issued in the form of anomalies, which are departures from the
20 average over a specified multiyear reference period (climatology). The model climatology is
21 estimated as the average of the retrospective forecasts over the hindcast period. However,
22 different operational centers that provide seasonal ensemble predictions use different hindcast
23 periods based on their model climatology. Additionally, the hindcast periods of recently
24 developed and upgraded newer models have shifted in the recent years. In this paper, we discuss
25 the recent challenges faced by APCC multi-model ensemble (MME) operations, especially
26 changes in the hindcast period for individual models. Based on the results of various experiments
27 for MME prediction, we propose changing the hindcast period, which is the most appropriate
28 solution for APCC operation. This makes the newly developed models join the MME and
29 increases the total number of participating models, which facilitates the skill improvement of the
30 MME prediction.

31

32 **Plain Language Summary**

33 In seasonal forecasting, it is well known that the MME, which combines different single-model
34 predictions from various operational and research centers, is a more effective way to improve
35 forecast skill. Since 2005, the APCC has provided the MME seasonal forecasts, and the models
36 participating in the APCC MME operations have been continuously changing. In particular, as
37 the hindcast periods of newly developed models shift to the latest, they cannot participate in
38 operational MME forecasts because of climatological discrepancies. However, over time, as the
39 number of new models expected to provide skillful forecasts gradually increases, the APCC
40 faces the challenge of continuously reducing the number of participating models or changing the
41 hindcast period to more recent years. Considering various aspects such as the number of
42 participating models, skills, and climatology period, we selected the most appropriate method for
43 APCC operation. Thus, the MME prediction skill has improved over most of the globe and
44 seasons because of the increase in the number of participating models, particularly the inclusion
45 of newer models.

46 **1 Introduction**

47 Seasonal forecasts are commonly expressed in terms of anomalies, as departures from the
48 climatological mean and/or probabilities of an event occurring with respect to a climatological
49 distribution (usually, tercile-based categorical forecasts). This allows users to see whether the
50 predicted seasonal mean variables are anomalously positive or negative with respect to
51 climatological means, and/or what probability of the events (e.g., above, near, or below-normal
52 category) is expected. Therefore, climatology is used as a benchmark or reference against which
53 the expected conditions are likely to be experienced. It also provides a way to remove systematic
54 biases in forecasts from dynamical prediction systems by subtracting model climatology, because
55 they are not perfect representations of the real world (Stockdale, 1997; Kumar et al., 2012). The
56 model climatology is estimated using retrospective forecasts (hindcasts) over a specified long-
57 term reference period.

58 World Meteorological Organization (WMO) recommends climatology (normals) to be
59 estimated as 30-year averages computed for the most-recent 30-year period finishing in a year
60 ending with 0 (WMO, 2007), i.e., 1991-2020 at present. National Meteorological and
61 Hydrological Services (NMHSs) estimate forecasts as departures from these 30-year normals in
62 their locations. However, different operational and research centers have different hindcast
63 periods resulting in the use of different climatology periods for model climatology. Furthermore,
64 the hindcast periods of recently developed and improved climate models, particularly beginning
65 of the hindcast period, tend to shift to recent years. The Asia-Pacific Economic Cooperation
66 (APEC) Climate Center (APCC) is one of the major operational centers providing well-validated
67 multi-model ensemble (MME) seasonal forecasts. Since its establishment in 2005, APCC has
68 collected dynamical ensemble forecasts through multi-institutional cooperation and coordinated
69 MME predictions. At present, 15 leading operational and research institutes from 11 countries
70 are involved in APCC operational MME prediction. MME operational centers, such as APCC
71 (Min et al., 2014, 2017), WMO Lead Center for Long-Range Forecast (WMO LC-LRF; Kim et
72 al., 2021), North American MME (NMME; Becker et al., 2014; Kirtman et al., 2014), and
73 Copernicus Climate Change Service (C3S; Manazanas et al., 2019) use a common hindcast
74 period for all participating models, which results in a relatively short period compared to that of
75 single-model prediction systems. For example, APCC used the hindcast period in the early 20

76 years covering from early-1980s to the mid-2000s and extended it to 28 years in 2019, 1983-
77 2010.

78 As the hindcast periods for recently developed newer models have gradually shifted to
79 later years, the full range of hindcast periods for the dynamical models routinely running in
80 operational centers has widened, from early-1980s to late-2010s nowadays. However, the
81 common hindcast period is rather short because of shift in the newer models' hindcast periods
82 beginning in the early 1990s. This raised a new issue at APCC, which combines all the
83 information from different climate prediction systems, particularly in 2019. This is because some
84 of the models included in the operational APCC MME prediction were expected to change to
85 their upgraded versions in 2020, and their hindcast periods shifted to more recent years. That is,
86 with the implementation of new models, if the common hindcast period, 1983-2010, were
87 maintained, the number of participating models in the MME would have been reduced and
88 would be gradually reduced in the future because recently developed models that are expected to
89 have better skills do not match this common hindcast period. This may lead to deterioration of
90 the MME prediction skill. Therefore, APCC has come to consider the issue of the hindcast
91 period, which could affect the number of participating models in the MME and eventually the
92 MME skill. This study discusses the challenges faced by MME operations caused by upgrading
93 participating models. In particular, we focus on the decrease in the number of participating
94 models in MME prediction with a shift to the later years of the hindcast periods of recently
95 developed models. We suggest the most appropriate solution for the APCC operation based on
96 several experiments with the different hindcast periods and different numbers of participating
97 models in the MME.

98

99 **2 Data and Method**

100 2.1 Forecast data

101 With the most recent joining of System 8 from Met France (METFR; [http://www.umr-
103 cnrm.fr/IMG/pdf/system8-technical.pdf](http://www.umr-
102 cnrm.fr/IMG/pdf/system8-technical.pdf)), APCC currently collects ensemble predictions from 15
104 state-of-the-art climate models, and the models are being continuously improved with great
efforts from their own operational and research centers. The MME prediction system largely

105 depends on operational changes for the modeling centers, and the participating models in the
106 MME operation for each year and season differ slightly depending on the operational situation at
107 that time. The collected models through the APCC multi-institutional cooperation for research
108 and operation purposes in 2019 and 2020 are listed in Table 1. In 2019, the operational MME
109 prediction comprised eight models from APCC (SCoPS; Ham et al., 2019), BOM (POAMA;
110 Cottrill et al., 2013), CWB (GFST119; Paek et al., 2015), JMA (MRI-CPS2; Takaya et al., 2018),
111 MSC/ECCC (CanSIP; Merryfield et al., 2013), NASA (GEOS-S2S-2; Molod et al., 2015), NCEP
112 (CFSv2; Saha et al., 2014), and PNU (CGCMv1.0; Ahn & Kim, 2013) that matched with the
113 common hindcast period of 1983-2010. The remaining six models could not be included in the
114 MME because of different hindcast periods, although some were recently upgraded, for example,
115 KMA (GloSea5GC2; Ham et al., 2019) and UKMO (GloSea5; MachLachlan et al., 2015).
116 Furthermore, several models were scheduled to be changed to their upgraded versions in 2020
117 (e.g., POAMA to ACCESS-S (Hudson et al., 2017) in BOM, SPSv2 to SPSv3 (Sanna et al.,
118 2017) in CMCC, and CanSIP to CanSIPv2 (Lin et al., 2020) in MSC/ECCC). To test sensitivity
119 in terms of predictability as the participating models in MME change due to their improvements,
120 we performed several experiments with varying reference periods and participating models in the
121 MME, where the MME forecast is a simple average of individual models with equal weights.

122

123 2.2 Verification data and Metrics

124 We focus on 1-month lead 3-month mean (seasonal) MME forecasts of 2m temperature
125 and precipitation over the globe (GL; 90°S-90°N) and sub-regions: Northern Extratropics (NE;
126 20°N-90°N), Southern Extratropics (SE; 20°S-90°S), Tropics (TR; 20°N-20°S), East Asia (EAs;
127 75°E-150°E, 15°N-60°N), South Asia (SAs; 60°E-140°E, 10°S-35°N), North America (NA;
128 190°E-310°E, 10°N-75°N), South America (SA; 270°E-330°E, 60°S-10°N), Australia (Aus;
129 110°E-180°E, 50°S-0°N), and Northern Eurasia (NEu; 25°E-190°E, 40°N-80°N). For skill
130 assessment, we use the National Center for Environmental Prediction (NCEP)-Department of
131 Energy (DOE) Reanalysis 2 data (Kanamitsu et al., 2002) for temperature and the Climate
132 Anomaly System and Outgoing Longwave Radiation Prediction Index data (CAMS-OPI,
133 Janowiak & Xie, 1999) for precipitation. For Nino 3.4 index, we use the optimum interpolation

134 (OI) version 2 monthly mean SST (Reynolds et al. 2002), obtained from the Climate Diagnostics
 135 Center of National Oceanic and Atmospheric Administration.

136 All model forecasts and observations were interpolated onto a 2.5 x 2.5 common grid.
 137 We used the anomaly pattern correlation coefficient (ACC) and temporal correlation coefficient
 138 (TCC) to assess the prediction skill. We used the ACC-based relative skill difference to assess
 139 the prediction skill improvement and deterioration of the MME forecasts with another model set
 140 compared to the reference model set. The statistical robustness of the skill difference was
 141 verified using a bootstrap resampling method with 500 Montel-Carlo simulations. This method
 142 involves estimating the distribution of a statistic by randomly resampling and using it to evaluate
 143 statistical significance (Wilks, 1995, 1997; Stephenson and Doblas-Reyes, 2000; Min et al. 2017).
 144 Student's t-test and the Mann-Kendall test (Mann, 1945; Kendall, 1975) were used to assess the
 145 statistical significance of the difference between means and trends of observations and
 146 predictions. All forecast data from individual models are expressed in the form of anomalies as
 147 departures from the model climatology. As verification data, we used observed anomalies to
 148 represent deviations from the observed climatology. Consequently, model bias does not affect
 149 forecast skill. However, the use of anomalies, which implies bias correction, enhances the role of
 150 the correct estimation of model and observed climatologies.

151

152 **Table 1.** Collected models through APCC multi-institutional cooperation in 2019 and 2020

Institute	2019		2020	
	Model	Hindcast Period	Model	Hindcast Period
APCC	SCoPS	1982-2013	SCoPS	1982-2013
BCC	CSM_1.1m	1991-2015	CSM_1.1m	1991-2015
BOM	POAMA	1983-2011	ACCESS-S	1990-2012
CMCC	SPSv2	1993-2016	SPSv3	1993-2016
CWB	GFST119	1982-2011	GFST119	1982-2011
HMC	SL-AV	1985-2010	SL-AV	1985-2010
JMA	MRI-CPS2	1979-2014	MRI-CPS2	1979-2014
KMA	GloSea5GC2	1991-2010	GloSea5GC2	1991-2016
MGO	MGOAM-2	1979-2004	MGOAM-2	1979-2004
MSC/ECCC	CanSIP	1981-2010	CanSIPv2	1981-2010
NASA	GEOS-S2S-2	1981-2016	GEOS-S2S-2	1981-2016
NCEP	CFSv2	1982-2010	CFSv2	1982-2010

PNU	CGCMv1.0	1980-2018	CGCMv1.0	1980-2019
UKMO	GloSea5	1993-2016	GloSea5	1993-2016

153 The bold text in 2019 indicates the models that participated in the operational APCC MME
 154 prediction based on 1983-2010 climatology.

155

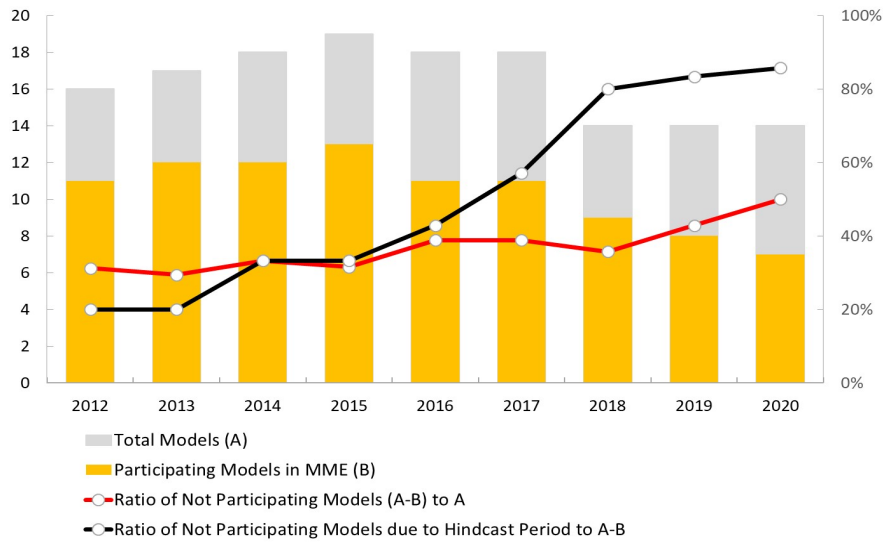
156 **3 Results**

157 More than two decades have passed since dynamical prediction systems have been
 158 operationally exploited for seasonal forecasting. Operational long-range forecasting centers make
 159 essential efforts to improve climate prediction systems. In particular, they tend to extend the
 160 period of hindcasts over which climatology is estimated and move it to more recent years. As
 161 shown in Fig. 1, the number of models providing ensemble forecasts to APCC and the number of
 162 models participating in the operational MME prediction vary from year to year, depending on the
 163 operational situations at the time. The proportion of models not included as part of the
 164 operational MME prediction has been gradually increasing and was expected to increase to
 165 nearly 50% by 2020 (red line in Fig. 1). Recently, the reason why some of the models could not
 166 participate in the MME has been mainly due to inconsistencies with the common hindcast period,
 167 and the proportion of these models has gradually increased over time (black line in Fig. 1). In
 168 other words, model developers continue to improve their model by gradually shifting their
 169 hindcast periods to more recent years. However, if the current common hindcast period for the
 170 APCC MME does not change, the number of models participating in APCC MME operation will
 171 gradually decrease. A more important issue is the MME skill, which is affected by the mean skill
 172 of individual models and models' diversity (Yoo & Kang, 2005; Alessandri et al., 2018). If the
 173 number of participating models in the MME prediction continues to decrease, particularly by
 174 excluding recently developed and improved newer models, it may lead to a decrease in MME
 175 skill.

176 When faced with this issue in 2019, APCC examined changes in MME skills if the
 177 common hindcast period was maintained, considering expected model changes scheduled for
 178 2020. As shown in Table 1, under the condition of the current 28-year hindcast period, the
 179 BOM's new model with a recent hindcast period (1990-2012), ACCESS-S, was expected to be
 180 unable to participate in the MME operation in 2020, and in the case of MSC/ECCC, CanSIP was

181 scheduled to be upgraded to CanSIPv2 with the 1981-2010 hindcast period. Therefore, it was
182 expected that CanSIPv2 would continue to participate in MME operations. To examine
183 differences in MME skill due to model changes, we compared the expected MME hindcast skill
184 with seven models in the 2020 version, considering BOM's and MSC/ECCC's model changes
185 (experiment), to the MME hindcast skill with eight models in the 2019 version (reference: APCC,
186 BOM, CWB, JMA, MSC/ECCC, NASA, NCEP, and PNU) for the common 28-year hindcast
187 period (1983-2010). We were able to perform the hindcasts of the new models scheduled to be
188 changed in 2020 because APCC collects a new version of the hindcast before the newer model is
189 applied to the MME operation and prepares various aspects from an operational perspective. Fig.
190 2 shows the relative skill difference of the experimental MME hindcast compared with that of
191 the reference MME hindcast. The ACC-based relative skill difference (%) was estimated as the
192 difference between the ACCs of the experimental and reference forecasts, divided by the ACC of
193 the reference forecasts. The relative skill difference is mainly negative, which indicates a
194 deterioration in the MME skill caused by the expected models' changes for 2020. The skill of
195 experimental forecasts for both global temperature and precipitation decreased across almost all
196 seasons. This is also true for the sub-regions in terms of 12-season averages (annual means), with
197 the exception of temperature in South America. That is, it was clearly expected that if the 28-
198 year hindcast period was maintained in 2020, the MME prediction skill would ultimately
199 decrease owing to a decrease in the number of participating models (from eight to seven), despite
200 the MSC ECCC's model being replaced by CanSIPv2, which has a higher prediction skill than
201 its previous version, CanSIP (Fig. 3). These results served as the motivation for the various
202 considerations and experiments in this study to increase the number of participating models and
203 consequently improve the MME prediction skill.

204

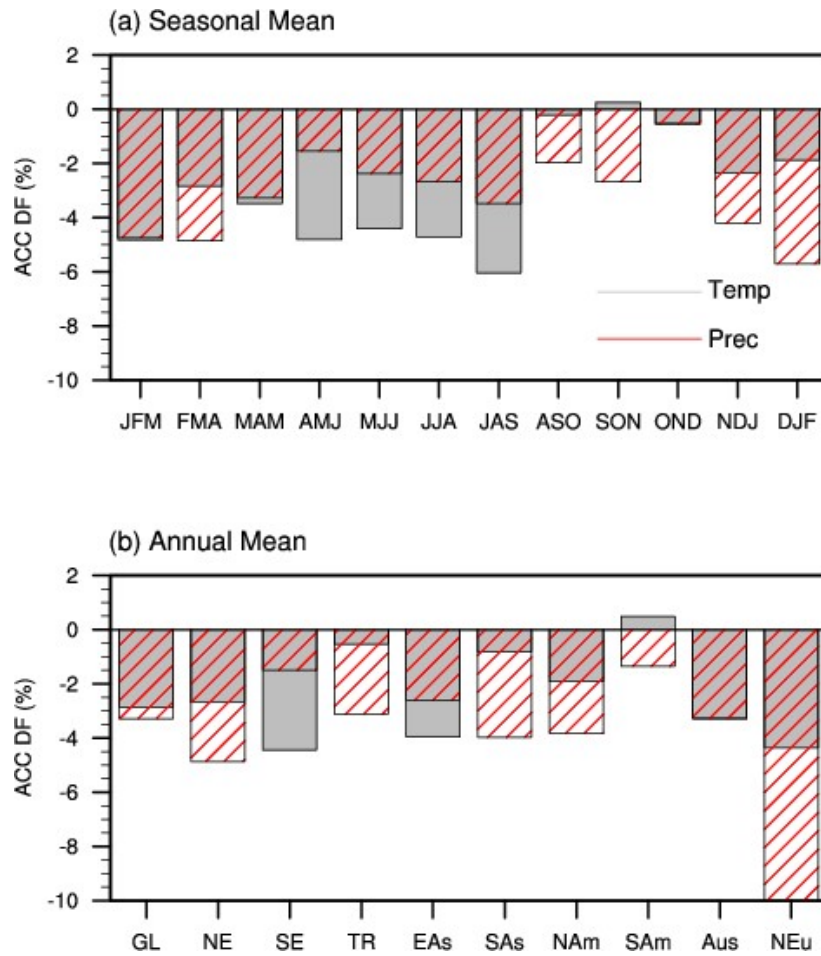


205

206 **Figure 1.** Changes in the number of models providing their seasonal forecasts to APCC (grey
 207 bar; A) and the number of models participating in the operational APCC MME prediction
 208 (yellow bar; B) in 2012-2020. Red lines indicate the proportion of models not participating in the
 209 operational MME prediction to the total models $((A-B)/A)$. Black lines represent the proportion
 210 of models not participating in MME due to inconsistency of common hindcast period to not
 211 participating models in MME. The values for 2020 refer to the expected changes if the 28-year
 212 (1983-2010) hindcast period for MME prediction continues in 2020.

213

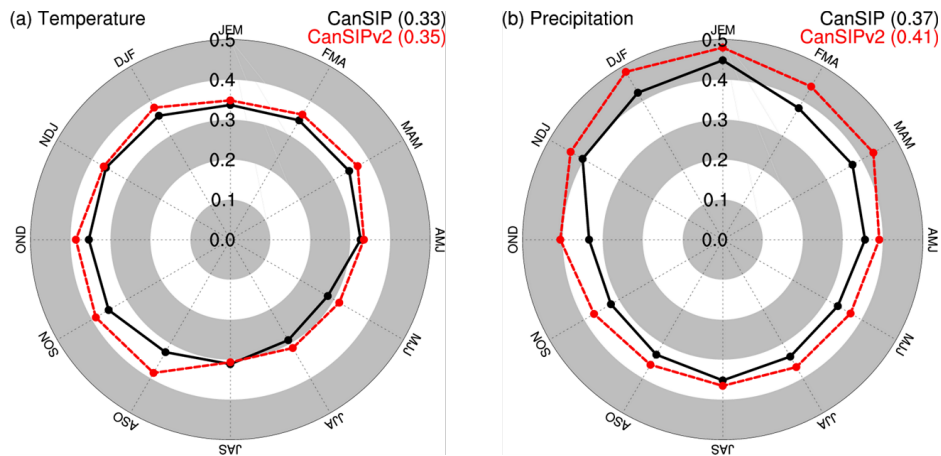
214



215

216 **Figure 2.** (a) Relative skill difference of the experimental MME hindcasts in 2020 to the
 217 reference MME hindcasts in 2019 of 3-month (seasonal) mean temperature and precipitation
 218 forecasts over the globe and (b) 12-season averaged (annual mean) forecasts for several sub-
 219 sub-regions for the common period of 1983-2010.

220



221

222 **Figure 3.** Anomaly pattern correlation coefficients (ACCs) for seasonal mean temperature and
 223 precipitation forecasts over the globe of CanSIP and CanSIPv2 for the common period of 1983-
 224 2010. The annual mean ACCs for each model are shown in parentheses.

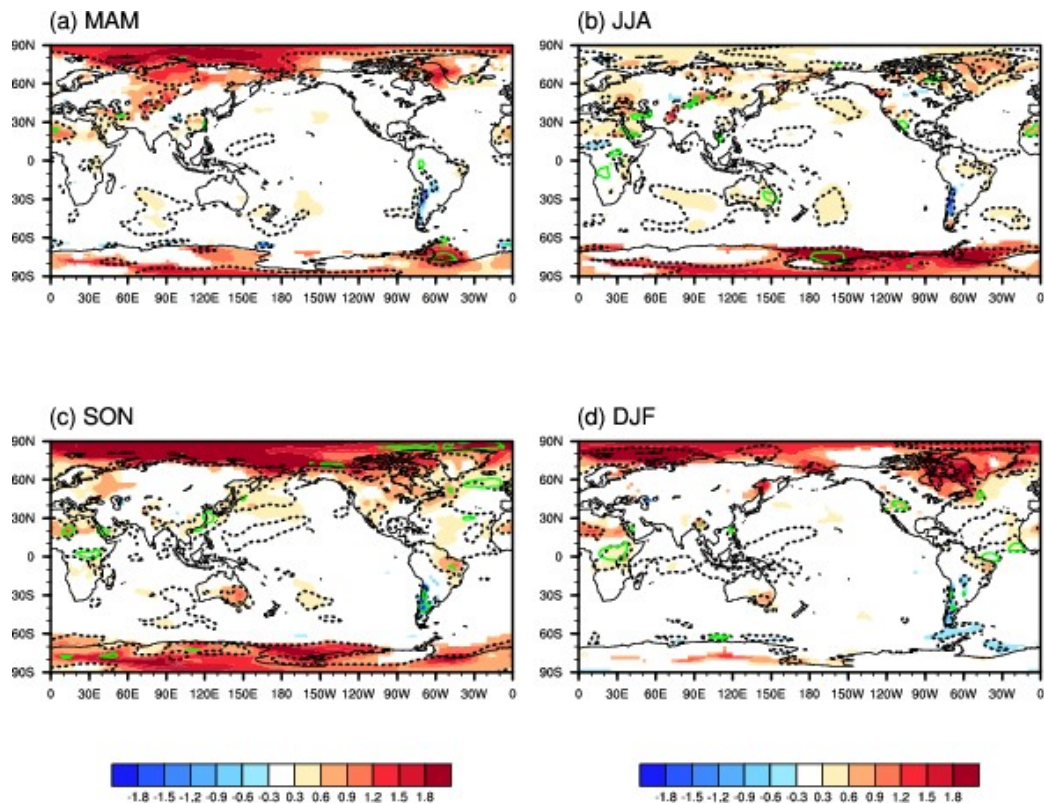
225

226 APCC considered several solutions to solve this hindcast issue and took advantage of a
 227 large set of models participating in the MME prediction. The first solution would be the use of
 228 forecast anomalies with respect to climatologies estimated over the models' own hindcast
 229 periods, which vary among the groups producing the model forecast, such as the IRI ENSO
 230 forecast (http://iri.columbia.edu/our-expertise/climate/forecasts/enso/current/?enso-sst_table).
 231 That is, all models can participate in MME prediction by using forecast anomalies with respect to
 232 different base periods and, consequently, to the different climatologies. However, discrepancies
 233 may arise if the climatologies differs significantly. We assessed the significance of the difference
 234 between climatologies estimated over two periods, 1983-2010 and 1993-2016, which covered the
 235 common hindcast period and the most recent hindcast period of the 14 models in the 2019
 236 version, at a 10% significance level based on the Student's *t*-test. The results showed that the
 237 differences between the two climatologies of seasonal mean temperature in the observation were
 238 statistically significant in many regions (Fig. 4). The most significant differences were evident in
 239 the high latitudes of the Northern and Southern Hemispheres throughout all seasons. In these
 240 regions, global warming has significantly accelerated in recent years. This is also evident in the
 241 South Indian Ocean in MAM and JJA and in the Western Pacific in SON and DJF. Furthermore,
 242 for the model with the longest hindcast period spanning from the early 1980s to the most recent
 243 years, the differences between climatologies from the periods 1983-2010 and 1993-2016 were

244 also statistically significant (not shown). Thus, the first solution may cause another issue in
245 forecast anomalies because of the significant differences in climatologies due to the different
246 reference (hindcast) periods of individual models, and eventually in the MME prediction that
247 combines the forecast anomalies of individual models (Wallace & Arribas, 2012). Furthermore,
248 this solution is not suitable for users who utilize our seasonal forecasts, such as, NMHSs. Users
249 formulate their local forecasts in terms of anomalies with respect to their local normals estimated
250 over the 30-year period appointed/defined by WMO. As a rule, for their local area of interest,
251 they perform corrections to MME forecasts to account for the difference between the normals
252 estimated over, e.g., 1991-2020 and MME climatology estimated over, e.g., 1983-2010.
253 However, this solution does not provide a reference for the MME climatology period, which may
254 confuse users performing regional/local corrections.

255 The second solution would be to separate the models into two groups, with hindcast
256 periods specific to each group, and the difference in climatology between the two groups should
257 not be significant. Climatology-I is specified for the current common hindcast period (1983-
258 2010) covered by most models so far. The common hindcast period covered by the newer models
259 (1993-2010) is specified as Climatology-II. As shown in Fig. 4, the difference between
260 Climatology-I and II is not statistically significant most of the globe and seasons. This indicates
261 that the newly developed and recently upgraded models may participate in MME prediction
262 using Climatology-II. This is slightly different from the first solution, as the difference between
263 the two climatologies is not statistically significant, which can reduce some of the confusion in
264 the user's post-processing and interpretation of our forecasts. However, another issue arises as to
265 which a reference period should be applied to observations to assess the MME forecasts
266 combined with two groups of models using different climatologies.

267



268

269 **Figure 4.** Differences between two climatologies over the period 1983-2010 and 1993-2016
 270 (black dashed line) and trends of observed seasonal mean temperature for the entire 34-year
 271 period 1983-2016 (shading). Differences and trends were only displayed at a 10% significance
 272 level using Student's t-test and Mann-Kendall test. The green lines represent statistically
 273 significant differences in the climatology between the 1983-2010 and 1993-2010 periods.
 274

275 In this situation, we suggest an alternative solution that is to change the current hindcast
 276 period to a unified 1991-2010, for which almost all models could be included. Models of CMCC
 277 and UKMO, starting with data from 1993, were treated as missing values for 1991-1992 to allow
 278 more models to participate in the MME and extend the hindcast period by at least 20 years.
 279 According to the guidelines for objective seasonal forecasting by WMO (2020), hindcast periods
 280 shorter than about 20 years may suffer from inadequate sample sizes to allow a robust estimation
 281 of skill. In addition, it was mentioned that a shorter hindcast period impacts the merging of
 282 information coming from different models using different hindcast periods, especially for MME
 283 approaches, because the anomalies and forecast quality are calculated with respect to the
 284 hindcast period. Additionally, in terms of prediction skill, increasing the number of participating
 285 models, by treating the 2-year period as missing for both models, had a positive effect on

286 improving the MME hindcast skill (not shown). To estimate the forecast skill according to the
 287 changes in the number of participating models as the hindcast period for MME climatology
 288 changes to unified 1991-2010, we further examined the skill of the MME hindcast in three
 289 different model combinations within the model suites of the 2020 version in Table 1. Table 2
 290 shows detailed descriptions of the three different model sets of the MME experiments. Here, 7M
 291 was composed of the same models as the experimental MME hindcast results based on the 28-
 292 year climatology shown in Fig. 2. However, in this experiment, the 20-year climatology was
 293 used to compare the MME prediction skill with all models, including the newly joined models
 294 owing to the change in the hindcast period to 1991-2010.

295

296 **Table 2.** Description of three different model suites of MME hindcasts in the 2020 version.

Experiment	Description
7M	7 models expected to continuously participate in MME for 2020 if the current 1983-2010 hindcast period is maintained (APCC, CWB, JMA, MSC/ECCC, NASA, NCEP, PNU)
+6M	Additional 6 models expected to newly participate in MME for 2020 by changing the hindcast period to unified 1991-2010 (BCC, BOM, CMCC, HMC, KMA, UKMO)
13M	All 13 models expected to participate in MME for 2020 by changing the hindcast period to unified 1991-2010

297

298 Under the condition of the 1991-2010 hindcast period, the diagrams shown in Fig. 5a and
 299 b demonstrate that the skills of the MMEs based on 7M (MME_7M) and +6M (MME_+6M)
 300 were comparable, showing ACC=0.36 (0.44) for annual mean temperature (precipitation) for
 301 both MMEs. By changing the hindcast period to 1991-2010, the MME consisting of all 13
 302 models (MME_13M) clearly outperformed MME_7M and MME_+6M for both temperature and
 303 precipitation over all 12 seasons. The skill improvement of MME_13M forecasts compared with
 304 that of MME_7M for both annual mean temperature and precipitation appears not only in the
 305 oceans but also on land, with the exception of precipitation in the Arctic region (Fig. 6), where
 306 the precipitation is relatively low, and there is significant uncertainty in observations.
 307 Consequently, the decrease in forecasting skill for precipitation in this region was not
 308 considered a significant concern in the paper. Most of these skill improvements in terms of

309 temporal correlation coefficients demonstrated statistical robustness at the 10% significance level
310 in a bootstrap test with 500 Monte-Carlo simulations, particularly evident in regions where the
311 prediction skills are relatively low.

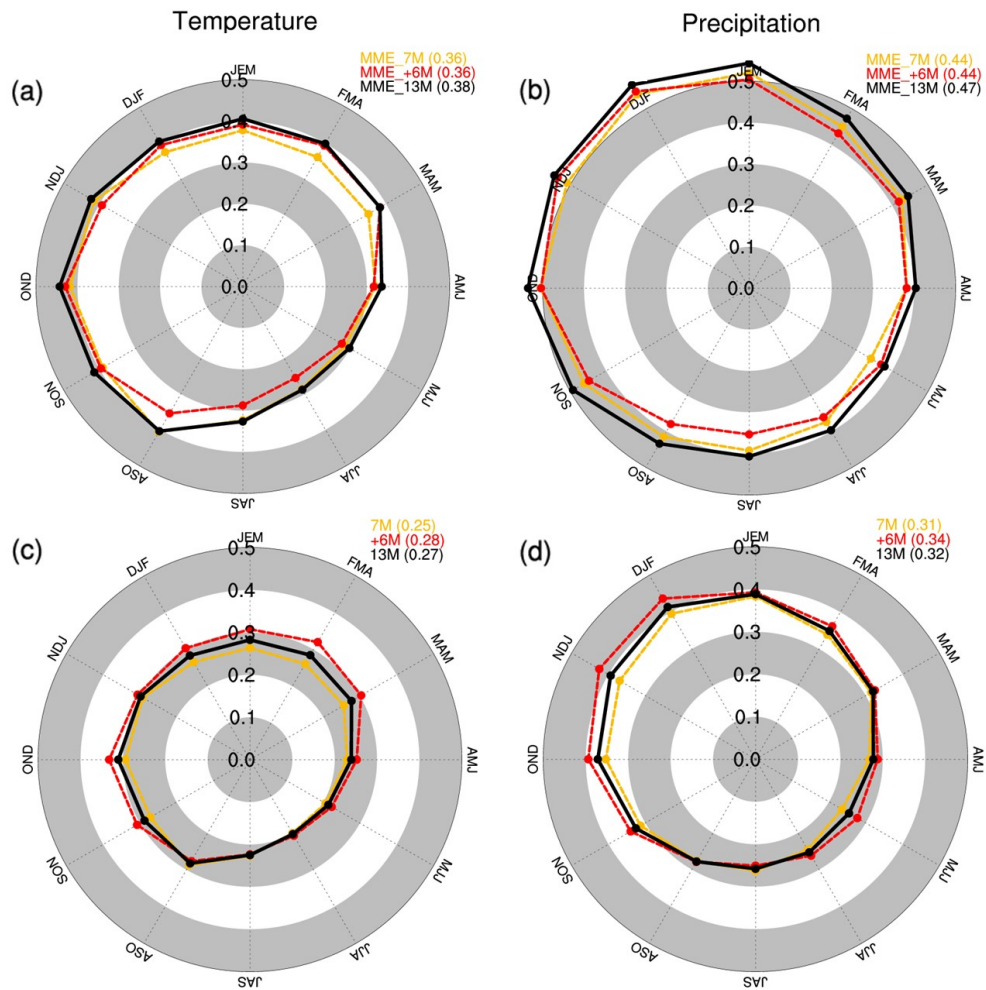
312 To conduct a detailed examination across seasons and regions, we calculated the ACC-
313 based relative skill difference between the MME_13M and MME_7M for each season and
314 region (Fig. 7). Our analysis revealed a notable enhancement in the forecast skill of MME_13M
315 for temperature during boreal winter seasons, demonstrating its statistical robustness. Notable
316 from a regional perspective, improvements beyond the tropical Pacific are significant, for
317 example, North America for temperature and East Asia, South America and Australia for
318 precipitation. There is variation in skill improvement across seasons and variables. Although the
319 details of this finding are beyond the scope of this study, a potential explanation lies in the
320 inclusion of three models within +6M: UKMO's GloSea5, KMA's GloSea5GC2, and BOM's
321 ACCESS-S, the latter two being developed based on UKMO's GloSea5. It is widely recognized
322 that GloSea5-based models exhibit similar overall model biases and prediction skills. Notably,
323 these models demonstrate high performance in predicting Northern extratropical atmospheric
324 circulation (e.g., Kang et al., 2014; MacLachlan et al., 2015; Scaife et al., 2014; Ham and Jeong,
325 2021) and the associated temperatures (e.g., Kryjov & Min, 2016; Lim et al., 2019). These
326 findings significantly enhance the forecast skill of MME_13M for boreal winter temperature.
327 However, the improvement in MME_13M prediction skill for summer temperatures was minimal
328 compared to winter, as +6M showed limited improvement in predicting summer temperatures.
329 Conversely, improvements in precipitation were robust across most seasons, with particularly
330 significant enhancements observed during boreal summer seasons. For precipitation, the greatest
331 variability is observed in tropical regions, where it is closely linked to convective activity
332 influenced by ENSO conditions (e.g., Ropelewski and Halpert, 1987; Collins et al., 2010).
333 Consequently, the largest model errors typically occur during spring and summer, particularly
334 when SST forcing is weak or during the ENSO transition phase (e.g., Jin et al. 2008; Wang et al.,
335 2009; Min et al., 2017). In contrast, the strong manifestation of ENSO conditions tends to occur
336 during winter, leading to already commendable accuracy in winter precipitation forecasts, even
337 with older models. In such situation, when the precipitation forecasting skill of +6M is moderate
338 across all seasons, the improvement in precipitation of MME_13M appears to be more

339 significant during the boreal summer seasons, when prediction skill is relatively lower, compared
340 to winter.

341 Consequently, these skill improvements of MME_13M were mainly due to the higher
342 mean skill of the newly participating models (+6M; mostly recently developed/upgraded models)
343 to MME by changing the hindcast period, compared to the mean skill of the originally
344 participating models (7M) for both temperature and precipitation across all seasons (Fig. 5c, d).
345 In addition, MME_13M, which represents a moderate level when averaging the skills of all 13
346 models, showed the highest skill because of the increase in the number of models and the
347 corresponding increase in the diversity of the contributing models (Yoo & Kang, 2005;
348 Alessandri et al., 2018). In other words, by changing the hindcast period to the unified 1991-
349 2010, models with relatively high skill can contribute to the MME, which can increase the total
350 number of participating models in the MME and ultimately improve the MME efficiency,
351 thereby improving the prediction skill of MME_13M compared to MME_7M.

352 Based on the results of the hindcast experiments, we changed the common base period to
353 1991-2010 for APCC MME operation from 2020, which is covered by almost all the models
354 (Oper). Finally, we assessed the MME skills of real-time forecasts from 2020JFM to 2023JAS
355 using the most recently updated observations. Real-time forecast verification is important for
356 operational centers to assess whether skill improvement exists in real-time forecasts as well as in
357 hindcasts, although this period is too short for the collection of a sufficient number of real-time
358 forecasts to obtain well-grounded conclusions. We first assessed Oper's forecast skill for both
359 variables, indicating a strong dependence on ENSO strength, which reaches its peak in boreal
360 winter and serves as one of the key sources of predictability for seasonal forecasts (Fig. 8a;
361 Wang et al. 2009; Barnston et al. 2010; Min et al. 2017). For example, relatively high levels of
362 the forecast skills were observed during the boreal autumn and winter seasons of 2020/21 and
363 2021/22, coinciding with moderate La Nina events. Towards mid-2023, a strong El Nino was
364 developing, accompanied by an improvement in forecasting skill. Meanwhile, in 2022 the strong
365 negative Nino 3.4 SST anomaly persisted into spring, summer, and autumn, providing strong
366 persistent forcing that governed skillful seasonal forecast. Conversely, the relatively low skills
367 were observed during the transition and/or ENSO-neutral phases of 2020, 2021 and 2023. For
368 comparison, we produced MME forecasts for the same periods as the models that would have
369 participated in the MME if the 1983-2010 hindcast period had not changed (Exp). By changing

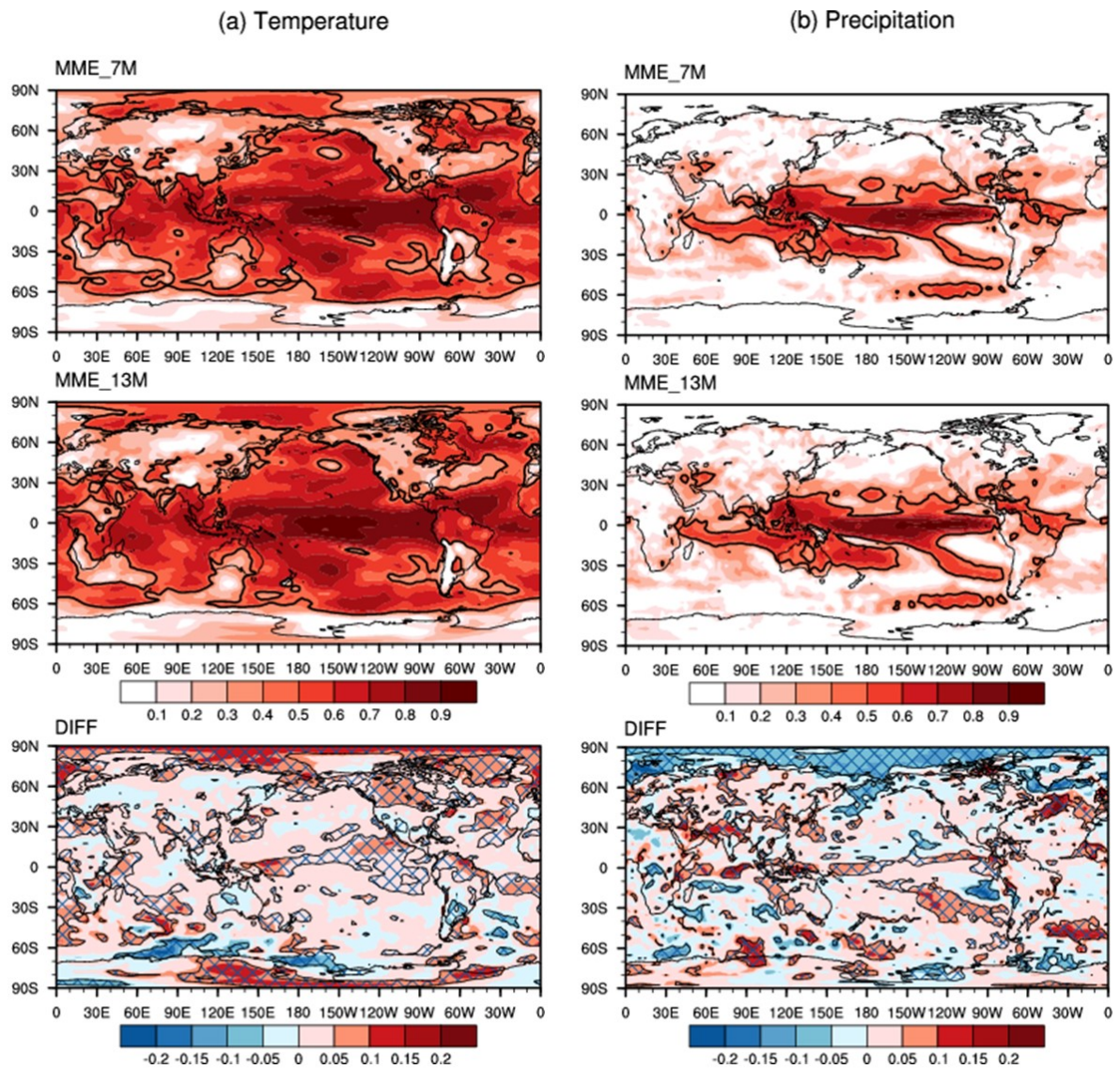
370 the hindcast period to 1991-2010, the number of participating models in the real-time MME
371 operations in 2020JFM-2023JAS increased by 100%, and the difference between Oper and Exp
372 gradually widened (Fig. 8b). The improvement or degradation in forecast skill by Oper fluctuates
373 across seasons and years under limited data set conditions. However, an encouraging finding for
374 real-time forecasts is the significant enhancement in Oper manifested from mid-2022, coinciding
375 with a widening disparity in the number of participating models between Oper and Exp. That is,
376 as the models continued to improve, along with the hindcast period shifted, it was clear that if the
377 1983-2010 hindcast period had been maintained, the number of participating models in the MME
378 operations would have gradually decreased, leading to a subsequent decline in forecast skill. As a
379 result, from the preliminary results of the real-time forecasts, substantial improvements in
380 temperature over the globe have been observed in recent years; however, the prediction of
381 precipitation still remains a difficult problem, with little change on a global scale (Fig. 8c). Given
382 that the assessment for real-time forecast has been based on limited data, more detailed analysis
383 is needed to determine the causes of the improvement and decrease in forecast skill for further
384 study as more data become available. Based on the results from hindcasts and real-time forecasts,
385 the change in the common hindcast period to 1991-2010 for MME prediction in 2020 was an
386 appropriate action for APCC operation from a long-term perspective.



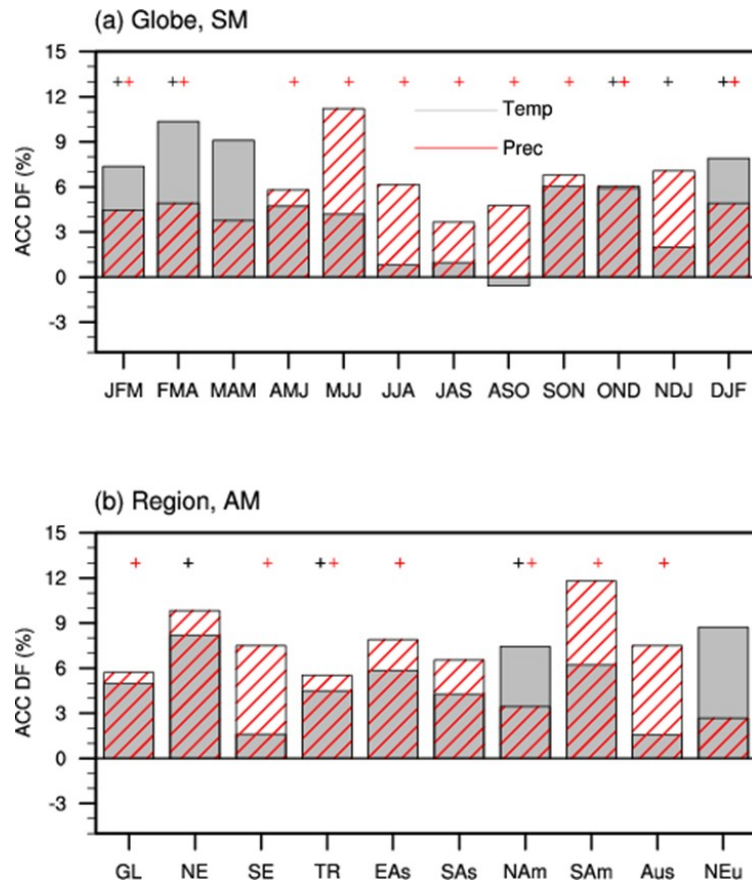
387

388 **Figure 5.** (a, b) ACCs of MME hindcasts (1991-2010) with different model combinations
 389 (MME_7M, MME_+6M, and MME_13M) and (c, d) average ACCs of the participating models
 390 for each combination (7M, +6M, and 13M), for seasonal mean temperature and precipitation
 391 forecasts over the globe. The annual mean ACCs for each MME and the average of models'
 392 skills are shown in parentheses.

393

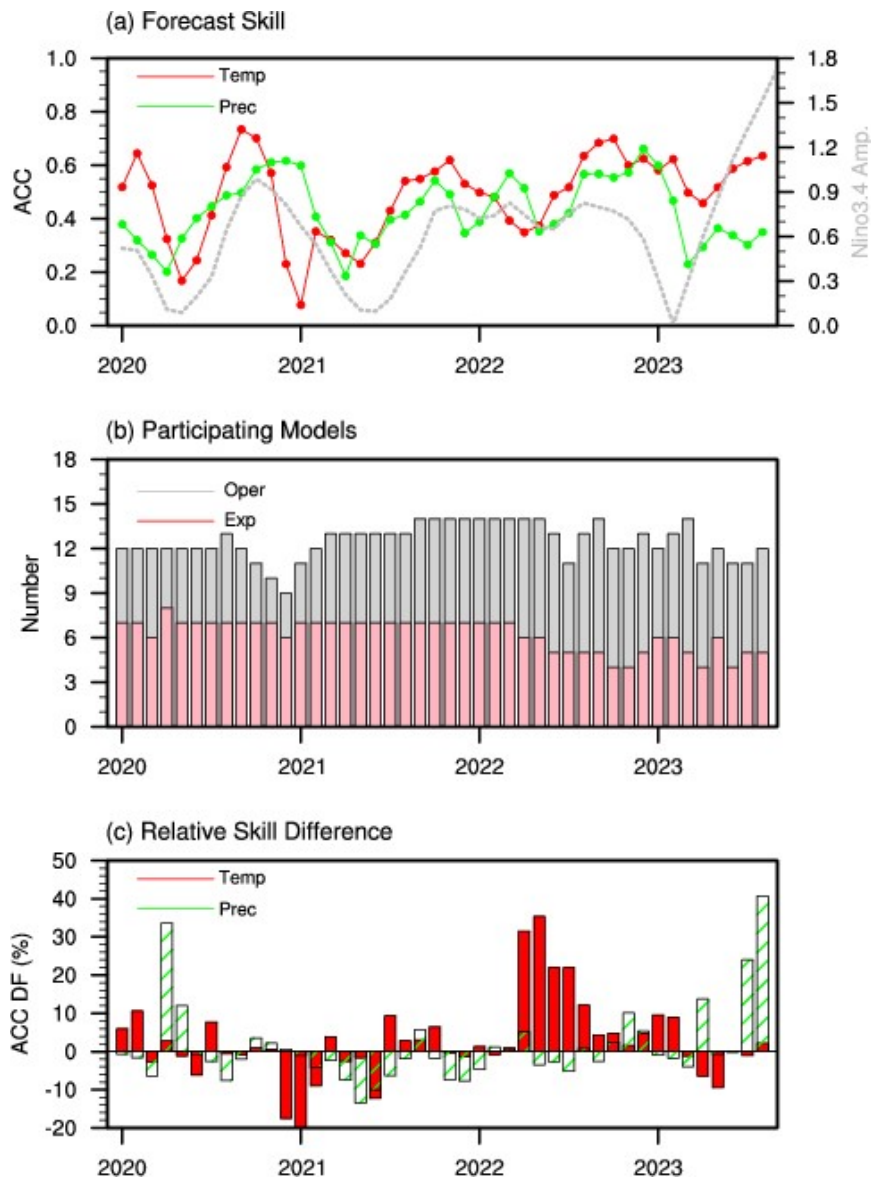


394
 395 **Figure 6.** Spatial distributions of annual mean temporal correlation coefficients (TCCs) for the
 396 MME hindcast (1991-2010) with 7 models (MME_7M) and 13 models (MME_13) of seasonal
 397 mean temperature and precipitation. The contour lines enclose the areas in which the TCCs are
 398 statistically significant at the 5% level using a two-tailed Student's t-test. The skill differences
 399 (DIFF) indicate the differences between the two MMEs (MME_13M minus MME_7M), with the
 400 skill difference being statistically robust at the 10% significance level in a bootstrap test with 500
 401 Monte-Carlo simulations.
 402



403

404 **Figure 7.** (a) ACC-based relative skill difference of MME_13M hindcasts to MME_7M
 405 hindcasts of seasonal mean temperature and precipitation forecasts over the globe and (b) annual
 406 mean forecasts for several sub-regions for the period of 1991-2010. The black and red crosses
 407 mark the seasons and regions for which the relative skill difference is statistically robust at the
 408 10% significance level in a bootstrap test with 500 Monte-Carlo simulations.



409

410 **Figure 8.** (a) ACCs of real-time operational MME forecasts (Oper) for global temperature and
 411 precipitation for 2020JFM-2023JAS. The grey line indicates the amplitude (absolute value) of 3-
 412 month mean Nino 3.4 Index. (b) Number of participating models in Oper and experimental
 413 forecasts (Exp) and (c) Relative skill difference of ACCs from Exp to Oper for global
 414 temperature and precipitation.

415

416 4 Conclusions

417 The construction of the MME is a compromise between the number of participating
 418 models and the length of the common hindcast period. An increase in the number of participating

419 models with sufficient model diversity decreases random and model formulation errors in MME
420 forecasts (e.g., DelSole et al., 2014; Yang et al., 2016). On the other hand, an increase in the
421 length of the common hindcast period decreases errors in climatology but increase random and
422 model formulation errors because of a decrease in the number of participating models in the
423 MME prediction (e.g., Shi et al., 2015). In this situation, as the hindcast periods of recently
424 developed and improved models have shifted to the latest, APCC faced new challenges in 2019
425 while continuing to maintain a common hindcast period for many years. As a result, the
426 proportion of models that could not participate in operational MME prediction was expected to
427 be approximately 50% by 2020 because their hindcast periods started in the mid-1980s to early
428 1990s. Based on the results of several experiments, we proposed a solution to change the
429 common hindcast period to a unified 1991-2010, which is the most appropriate method for
430 APCC operation, reflecting recently developed models. That is, by changing the reference period
431 for MME prediction, APCC provides opportunities for participation in operational MME
432 prediction for newly developed/upgraded models, resulting in a double increase in the number of
433 participating models and improvement in the MME prediction skill.

434 However, some questions remain regarding whether the 20-year hindcast period is
435 sufficient to represent the climatological means. Because the operational MME center
436 incorporates predictions from various models, it is inevitable that the hindcast period for the
437 MME is shorter than that for individual models. The suggested 20-year climatology is
438 comparable to the climatologies of other MME groups for seasonal forecasting (e.g., WMO LC-
439 LRF (1993-2009; 17 years) and C3S (1993-2016; 24 years)). Although WMO recommends that
440 the hindcast period should be as long as possible (WMO, 2019) and that a short period may
441 affect the estimation of anomalies and forecast skill of MME, especially those that integrate
442 predictions from various models, even the WMO LC-LRF currently uses a common 17-year
443 hindcast period in performing MME by integrating outputs from 16 Global Producing Centres'
444 (GPC) models. That is, there are still realistic limitations or gaps in the hindcast period of
445 producing centers that match the WMO recommendation. The differences in hindcast periods for
446 each model mainly stem from when the models were developed and the production schedule for
447 its operation. For example, the hindcast period of recently developed models has shifted to more
448 recent years, whereas the hindcast period of models that were developed relatively early and
449 have continued to be maintained mostly covers the hindcast period of 1980s to mid-to-late 2010s.

450 Moreover, in terms of the production schedules, some systems follow a so-called “on the fly”
451 approach, generating a new set of hindcasts every time a new forecast is produced (e.g., PNU).
452 In some models, fixed hindcasts are produced before the system becomes operational and remain
453 unchanged throughout its operational lifetime (e.g., NCEP). Each method has its own advantages,
454 and each modeling center produces hindcasts in a manner that is appropriate for their operational
455 situation. This issue can be fundamentally solved by making further efforts to extend or shift the
456 hindcast period at each modeling center, along with improvements in other modeling
457 components. As part of these efforts, APCC, as one of the MME model providers, is currently
458 working to expand the period for the APCC’s in-house model, SCoPS, to mid to late 2010s.
459 Another aspect of the APCC’s efforts as an MME center is to encourage MME model providers
460 to expand the hindcast period to the latest through regularly held APCC MME Model Providers’
461 Meetings. However, these problems cannot be solved in a short time and may not be feasible on
462 the operational situation of each modeling center. In this situation, this study is significant in that
463 we addressed the critical and practical challenges recently faced by operational MME centers
464 due to the hindcast issue and provided various approaches that MME groups can consider to
465 solve these problems.

466 Finally, although not within the scope of this study, the most important issue in recent
467 years is that since late 2021, NMHSs worldwide have used the WMO recommended 1991-2020
468 normals ([https://www.wmo.int/edistrib_exped/grp_prs/_en/08791-2019-CLW-CLPA-DMA-
469 CLIN8110_en.pdf](https://www.wmo.int/edistrib_exped/grp_prs/_en/08791-2019-CLW-CLPA-DMA-CLIN8110_en.pdf)). However, there are still some limitations to matching with the WMO-
470 recommended normal period; currently no climate center providing MME seasonal forecasts to
471 the NHMSs uses a climatology matching with the WMO references. In particular, the recent
472 period in which the difference between the model climatology (e.g., 1991-2010) and the WMO
473 normal (e.g., 1991-2020) appears is the period when global warming is accelerating. Therefore,
474 forecast anomalies based on a more recent reference climate may be more relevant in the context
475 of climate change (WMO, 2020). It is more difficult to make seasonal forecasts during periods of
476 strong climate trends, and the warming trends are important effects that should not be discarded.
477 Therefore, further studies needed on the methodologies for adjusting and correcting (or
478 calibrating) the climatology in models to the WMO normal, including recent periods.

479

480 **Acknowledgments**

481 This study was supported by APEC Climate Center. The authors acknowledge the APCC MME
482 Producing Centres (PCs) for making their hindcast/forecast data available for analysis and the
483 APCC for collecting and archiving them and for organizing the APCC MME prediction. We also
484 thank the APCC MME PCs for discussing this issue at the 3rd APCC MME Providers' Meeting
485 in 2019.

486

487 **Data Availability Statement**

488 The single-model and MME predictions used in this study are available from the Climate Service
489 Integration Platform, Climate Information toolkit (CLIK; <https://cliks.apcc21.org>). The National
490 Center for Environmental Prediction – Department of Energy (NCEP-DOE) reanalysis 2 was
491 obtained from the NOAA/OAR/ESRL PSD, Boulder, Colorado, USA (available online at
492 <https://psl.noaa.gov/data/gridded/index.html>). The monthly precipitation was acquired from the
493 NOAA/NCEP climate anomaly monitoring system – outgoing longwave radiation precipitation
494 index (CAMS OPI; available online at
495 https://www.cpc.ncep.noaa.gov/products/global_precip/html/wpage.cams_opi.html). For Nino
496 3.4 index, we use the optimum interpolation (OI) version 2 monthly mean SST (OI SSTv2;
497 available online at <https://www.psl.noaa.gov/data/gridded/data.noaa.oisst.v2.html>).

498 **References**

- 499 Ahn, J. B., & Kim, H. J. (2013). Improvement of one-month lead predictability of the wintertime
500 AO using a realistically varying solar constant for a CGCM. *Meteorological Applications*,
501 21(2), 415-418. <https://doi.org/10.1002/met.1372>
- 502 Alessandri, A., Catalano, F., Lee, J. Y., Wang, B., Lee, D. Y., Yoo, J. H., & Weisheimer, A.
503 (2018). Grand European and Asian-Pacific multi-model seasonal forecasts: maximization
504 of skill and of potential economical value to end-users. *Climate Dynamics*, 50, 2719-2738.
505 <https://doi.org/10.1007/s00382-017-3766-y>
- 506 Barnston, A. G., Shuhua, L., Mason, S. J., DeWitt, D. G., Goddard, L., & Gond, X. (2010)
507 Verification of the first 11 years of IRI's seasonal climate forecast. *Journal of Applied*
508 *Meteorology and Climatology*, 49, 493-520. <https://doi.org/10.1175/1520->
509 0493(2003)131<1509:SAIVOT>2.0.CO;2
- 510 Becker, E., den Dool, H. V., & Zhang, Q. (2014). Predictability and forecast skill in NMME.
511 *Journal of Climate*, 27(15), 5891-5906. <https://doi.org/10.1175/JCLI-D-13-00597.1>
- 512 Collins, M., An, S. I., Cai, W., Ganachaud, A., Guilyardi, E., Jin, F. F., Jochum, M., Lengaigne,
513 M., Power, S., Timmermann, A., Vecchi, G., & Wittenberg, A. (2010). The impact of
514 Global Warming on the Tropical Pacific Ocean and El Nino. *Nature Geoscience*, 3(6),
515 391-397.
- 516 Cottrill, A., Hendon, H. H., Lim, E.-P., Langford, S., Shelton, K., et al. (2013). Seasonal
517 forecasting in the Pacific using the coupled model POAMA-2. *Weather and Forecasting*,
518 28(3), 668-680. <https://doi.org/10.1175/WAF-D-12-00072.1>
- 519 DelSole, T., Nattala, J., & Tippett, M. K. (2014). Skill improvement from increased ensemble
520 size and model diversity. *Geophysical Research Letters*, 41, 7331-7342.
521 <https://doi.org/10.1002/2014GL060133>
- 522 Ham, H., Lee, S.-M., Hyun, Y.-K., & Kim, Y. (2019). Performance assessment of monthly
523 ensemble prediction data based on improvement of climate prediction system at KMA.
524 *Atmosphere*, 29(2), 149-164. <https://doi.org/10.14191/Atmos.2019.29.2.149>

- 525 Ham, S. Y., Im, A.-Y., Kang, S., Jeong, H., & Jeong, Y. (2019). Correction to : A newly
526 developed APCC ScoPS and its prediction of East Asia seasonal climate variability.
527 *Climate Dynamics*, 53, 3703-3704. <https://doi.org/10.1007/s00382-019-04894-y>
- 528 Ham, S. Y. And Jeong, Y (2021) Characteristics of subseasonal winter prediction skill
529 assessment of GloSea5 for East Asia. *Atmopshere*, 12(10), 1311.
530 <https://doi.org/10.3390/atmos12101311>
- 531 Hudson, D., Alves, O., Hendon, H. H., Lim, E.-P., et al. (2017). ACCESS-S1 The new Bureau of
532 Meteorology multi-week to seasonal prediction system. *Journal of Southern Hemisphere*
533 *Earth System Science*, 67(3). <https://doi.org/10.22499/3.6703.001>
- 534 Janowiak, J. E., & Xie, P. (1999). CAMS_OPI: a global satellite-raingauge merged product for
535 real-time precipitation monitoring applications [Dataset]. *Journal of Climatology*, 12(11),
536 3335-3342. [https://doi.org/10.1175/1520-0442\(1999\)012<3335:COAGSR>2.0.CO;2](https://doi.org/10.1175/1520-0442(1999)012<3335:COAGSR>2.0.CO;2)
- 537 Jin, E. K., Kinter III, J. L., Wang, B., Pack, C. K., Kang, I. S., Kirtman, B. P., Kug, J.-S., Kumar,
538 A., Juo, J.-J., Schemm, J., Sukla, J., & Yamagata T. (2008). Current status of ENSO
539 prediction skill in coupled ocean-atmosphere models. *Climate Dynamics*, 31(6), 647-664.
540 <https://doi.org/10.1007/s00382-008-0397-3>
- 541 Kang, D., Lee, M. I., Im, J., Kim, D., Kim, H. M., Kang, H. S., Schubert, S. D., Arribas, A., &
542 MacLachlan, C. (2014). Prediction of the Arctic Oscillation in boreal winter by dynamical
543 seasonal forecasting systems. *Geophysical Research Letters*. 41, 3577–3585.
544 <https://doi.org/10.1002/2014GL060011>
- 545 Kanamitsu, M., Ebisuzaki, W., Woollen, J., Yang, S.-K., Hnilo, J. J., Fiorino, M., & Potter, G. L.
546 (2002) [Dataset]. NCEP-DOE AMIP-II Reanalysis (R-2). *Bulletin of the American*
547 *Meteorological Society*, 83(11), 1631-1643. <https://doi.org/10.1175/Bams-83-11-1631>
- 548 Kendall, M. G. (1975). Rank Correlation Methods. New York, NY, Oxford University Press
- 549 Kim, G., Ahn, J. B., Kryjov, V. N., Lee, W. S., Kim, D. J., & Kumar, A. (2021). Assessment of
550 multi-model ensemble methods for WMO LC-LRFMME. *International Journal of*
551 *Climatology*, 41, E2462-E248. <https://doi.org/10.1002/joc.6858>.

- 552 Kirtman, B. P., Min, D., Infanti, J. M., et al. (2014). The North American Multimodel Ensemble:
553 Phase-1 Seasonal-to-Interannual Prediction; Phase-2 toward Developing Intraseasonal
554 Prediction. *Bulletin of the American Meteorological Society*, 95(4), 585-601.
555 <https://doi.org/10.1175/BAMS-D-12-00050.1>
- 556 Kryjov, V. N., & Min, Y.-M. (2016). Predictability of the wintertime Arctic Oscillation based on
557 autumn circulation. *International Journal of Climatology*, 36, 4181–4186.
558 <https://doi.org/10.1002/joc.4616>
- 559 Kumar, A., Chen, M., Zhang, L., Yang, W., Xue, Y., Wen, C., Marx, L., & Huang, B. (2012). An
560 analysis of the nonstationarity in the bias of sea surface temperature forecasts for the
561 NCEP Climate Forecast System (CFS) version 2. *Monthly Weather Review*, 140, 3003-
562 3016. <https://doi.org/10.1175/MWR-D-11-00335.1>
- 563 Lin, H., William, J., Muncaster, R., et al. (2020). The Canadian Seasonal to Interannual
564 Prediction System Version 2 (CanSIPv2), *Weather & Forecasting*, 35(4), 1317-1343.
565 <https://doi.org/10.1175/WAF-D-19-0259.1>
- 566 Lim, J., Dunstone, N. J., Scaife, A. A., and Smith D. M. (2019). Skillful seasonal prediction of
567 Korean winter temperature. *Atmospheric Science Letter*, 20, <https://doi.org/10.1002/asl.881>
- 568 MacLachlan, C., Arribas, A., Peterson, K. A., Maidens, A., Fereday, D., Scaife, A. A., Gordon,
569 M., Vellinga, M., Williams, A., Comer, R. E., Camp, J., Xavier, P., & Madec, G. (2015).
570 Global Seasonal forecast system version 5 (GloSea5): a high-resolution seasonal forecast
571 system. *Q. J. R. Meteorol. Soc.* 141, 1072–1084. <https://doi.org/10.1002/qj.2396>
- 572 Mann, H. B. (1945). Nonparametric tests against trend. *Econometrica*, 13(3), 245-259.
573 <https://doi.org/10.2307/1907187>
- 574 Manzanas, R., Gutierrez, J. M., Bhend, K., Hemri, S., Doblas-Reyes, F. J., Torralba, V., Penabad,
575 E., & Brookshaw, A. (2019). Bias adjustment and ensemble recalibration methods for
576 seasonal forecasting: a comprehensive intercomparison using the C3S dataset. *Climate*
577 *Dynamics*, 53, 1287-1305. <https://doi.org/10.1007/s00382-019-04640-4>

578 Merryfield, W. J., et al. (2013). The Canadian seasonal to interannual prediction system. Part I:
579 models and initialization. *Monthly Weather Review*, 141, 2910–2945. doi:10.1175/MWR-
580 D-12-00216.1

581 Min, Y. M., Kryjov, V. N., & Oh, S. M. (2014). Assessment of APCC multimodel ensemble
582 prediction in seasonal climate forecasting: Retrospective (1983-2003) and real-time
583 forecasts (2008-2013). *Journal of Geophysical Research: Atmospheres*, 119, 12,132-
584 12,150. <https://doi.org/10.1002/2014JD022230>

585 Min, Y. M., Kryjov, V. N., Oh, S. M., & Lee, H. J. (2017). Skill of real-time operational
586 forecasts with the APCC multi-model ensemble prediction system during the period 2008-
587 2015 [Dataset]. *Climate Dynamics*, 49(11–12), 4141–4156.
588 <https://doi.org/10.1007/s00382-017-3576-2>

589 Molod, A. M., Takacs, L. L., Suarez, M., & Bacmeister, J. (2015). Development of the GEOS-5
590 atmospheric general circulation model: evolution from MERRA to MERRA2.
591 *Geoscientific Model Development*, 8, 1339-1356. [https://doi.org/10.5194/gmd-8-1339-](https://doi.org/10.5194/gmd-8-1339-2015)
592 2015

593 Paek, H., Yu, J.-Y., Hwu, J.-W., Lu, M.-M., & Gao, T. (2015). A source of AGCM bias in
594 simulating the western Pacific subtropical high: Different sensitivities to the two types of
595 ENSO. *Monthly Weather Review*, 143(6), 2348-2362. [https://doi.org/10.1175/MWR-D-14-](https://doi.org/10.1175/MWR-D-14-00401.1)
596 00401.1

597 Reynolds, R. W., Rayner, N. A., Smith, T. M., Stokes, D. C., & Wang, W. (2002) An improved
598 in situ and satellite SST analysis for climate [Dataset]. *Journal of Climate*, 15, 1609-1625.
599 [https://doi.org/10.1175/1520-0442\(2002\)015<1609:AIISAS>2.0.CO;2](https://doi.org/10.1175/1520-0442(2002)015<1609:AIISAS>2.0.CO;2)

600 Ropelewski, C. F., & Halpert, M. S. (1987) Global and Regional Scale Precipitation Patterns
601 Associated with the El Nino/Southern Oscillation. *Monthly Weather Review*, 115(8), 1606-
602 1626. [https://doi.org/10.1175/1520-0493\(1987\)115<1606:GARSPP>2.0.CO;2](https://doi.org/10.1175/1520-0493(1987)115<1606:GARSPP>2.0.CO;2)

603 Saha, S., et al. (2014). The NCEP climate forecast system version 2. *Journal of Climate*, 27,
604 2185-2208. <https://doi.org/10.1175/JCLI-D12-00823.1>

605 Sanna, A., Borrelli, A., Pthasiadis, P., Materia, S., Storto, A., Tibaldi, S., & Gualdi, S. (2017).
606 CMCC-SPS3: the CMCC Seasonal Prediction System 3. Centro Euro-Mediterraneo sui
607 Cambiamenti Climatici. CMCC Tech. Rep. RP0285, p61

608 Scaife, A. A., Arribas, A., Blockley, E., Brookshaw, A., Clark, R. T., Dunstone, N., et al. (2014).
609 Skillful long-range prediction of European and North American winters. *Geophysical*
610 *Research Letter*, *41*, 2514-2519. <https://doi.org/10.1002/2014GL059637>

611 Shi, W., Schaller, N., MacLeod, D., Palmer, T. N., & Weisheimer, A. (2015). Impact of hindcast
612 length on estimates of seasonal climate predictability. *Geophysical Research Letters*, *42*(5).
613 doi:10.1002/2014GL062829

614 Stephenson, D. B., & Doblas-Reyes, F. J. (2000). Statistical methods for interpreting Monte
615 Carlo ensemble forecasts, *Tellus (A)*, *52*, 300–322. [https://doi.org/10.3402/tellusa.v52i3.](https://doi.org/10.3402/tellusa.v52i3.12267)
616 12267

617 Stockdale, T. N. (1997). Coupled ocean-atmosphere forecasts in the presence of climate drift.
618 *Monthly Weather Review*, *235*, 809-818. [https://doi.org/10.1175/1520-](https://doi.org/10.1175/1520-0493(1997)125<0809:COAFIT>2.0.CO;2)
619 0493(1997)125<0809:COAFIT>2.0.CO;2

620 Takaya, Y., Hirahara, S., Yasuda, T., Matsueda, S., et al. (2018). Japan Meteorological
621 Agency/Meteorological Research Institute-Coupled Prediction System version 2
622 (JMA/MRI-CPS2): atmosphere-land-ocean-sea ice coupled prediction system for
623 operational seasonal forecasting. *Climate Dynamics*, *50*(1), 1-15.
624 <https://doi.org/10.1007/s00382-017-3638-5>

625 Wang, B., et al. (2009) Advance and prospectus of seasonal prediction: assessment of the
626 APC/CliPAS 14-model ensemble retrospective seasonal prediction (1980-2004). *Climate*
627 *Dynamics*, *33*, 93-117. <https://doi.org/10.1007/s00382-008-0460-0>

628 Wallace, E., Arribas, A. (2012). Forecasting with reference to a specific climatology. *Monthly*
629 *Weather Review*, *140*, 3795-3802. <https://doi.org/10.1175/MWR-D-12-00159.1>

630 Wilks, D. S. (1995). *Statistical Methods in the Atmospheric Sciences*, 2nd ed. Elsevier Academic
631 Press: San Diego, CA.

632 Wilks. D. S. (1997). Resampling hypothesis tests for autocorrelated fields. *Journal of*
633 *Climatology*, 10, 65–82. [https://doi.org/10.1175/1520-0442\(1997\)010<0065:RHTFAF>](https://doi.org/10.1175/1520-0442(1997)010<0065:RHTFAF>2.0.CO;2)
634 2.0.CO;2.

635 WMO (2007). *The role of climatological normals in a changing climate*. WCDMP-No. 61,
636 WMO/TD-No. 1377, Geneva, World Meteorological Organization

637 WMO (2019) Manual on the Global Data-processing and Forecasting System. WMO-No. 485,
638 Geneva, Switzerland

639 World Meteorological Organization (2020). *Guidance on Operational Practices for Objective*
640 *Seasonal Forecasting*. WMO-No. 1246, Geneva, Switzerland

641 Yang, D., Yang, X. O., Xie, Q., Zhang, Y., Ren, X., & Tang, Y. (2016). Probabilistic versus
642 deterministic skill in predicting the western North Pacific-East Asian summer monsoon
643 variability with multimodel ensembles. *Journal of Geophysical Research-Atmosphere*,
644 121(3), 1079-1103. <https://doi.org/10.1002/2015JD023781>

645 Yoo, J. H., & Kang, I. S. (2005). Theoretical examination of a multi-model composite for
646 seasonal prediction. *Geophysical Research Letter*, 32, L18707.
647 <https://doi.org/10.1029/2005GL023513>